CLEAN
Soil Air Water

Enos W. Wambu[1,4]
Charles O. Onindo[1]
Willis Ambusso[2]
Gerald K. Muthakia[3]

[1]Department of Chemistry, Kenyatta University, Nairobi, Kenya
[2]Department of Physics, Kenyatta University, Nairobi, Kenya
[3]Department of Chemistry, Kimathi University College of Technology, Nyeri, Kenya
[4]Current address: Department of Chemistry, Bondo University College, Bondo, Kenya

Research Article

Removal of Fluoride from Aqueous Solutions by Adsorption Using a Siliceous Mineral of a Kenyan Origin

The problem of high fluoride in water sources in Africa and the rest of the developing world has exacerbated in the latest past due to increasing shortage of water. More people are being exposed to high water fluoride resulting in elevated levels of fluorosis in the societies. Fluoride (F) adsorption from solutions using a siliceous mineral from Kenya (M1) was studied on batch basis and results verified on high fluoride water using fixed-bed column experiments. About 100% batch F adsorption was achieved at 200 mg/L F concentration, 0.5 g/mL adsorbent dosage, 303–333 K, and pH 3.4 ± 0.2. Based on Giles classifications, F adsorption isotherm was found to be an H3 type isotherm. The equilibrium data was correlated to Freundlich and Langmuir models and the maximum Langmuir adsorption capacity was found to be 12.4 mg/g. Column experiments were conducted for different fluoride concentrations, bed depths, and flow rates. The F breakthrough curves were analyzed using the Thomas model and efficient F adsorption was found to occur at low flow rates and low influent concentrations. The Thomas F adsorption capacity (11.7 mg/g) was consistent with the Langmuir isotherm capacity showing that M1 could be applied as an inexpensive medium for water defluoridation.

Keywords: Batch adsorption; Breakthrough curve; Equilibrium isotherm; Fluorosis; Water quality

Received: March 28, 2011; *revised:* May 27, 2012; *accepted:* June 26, 2012

DOI: 10.1002/clen.201100171

1 Introduction

Although sufficient dietary fluoride (F) is essential for prevention of dental carries and normal functioning of body, regular intake of F above recommended levels [1] results in dental fluorosis among other ailments and at higher concentrations in skeletal fluorosis with chronic and fatal thresholds from 4 g [2]. The problem of high fluoride concentrations in water sources in Africa and the rest of the developing world has exacerbated in the latest past due to increasing shortage of water [3–5]. More people are being exposed to high water fluoride levels resulting in elevated levels of fluorosis in the societies [6].

Technologies for removal of fluoride from drinking water include: coagulation using alum [7], precipitation using lime [8], contact precipitation using calcium salts [9], electro-coagulation (EC) [10], electrodialysis (ED) [11], reverse osmosis (RO) [12], solar distillation [13], adsorption and ion-exchange [14], and membrane technology. Precipitation, contact precipitation and coagulation using metal salts are however inefficient and normally require high doses of reagents which results in large volumes of fluoride-laden sludge and associated sludge disposal problems; thus adding to the cost of treatment. Then, the level of residual coagulants and precipitants in treated water must be monitored carefully to ensure that it does not exceed standards for drinking water. RO, ED, EC, and membrane technology, on the hand, are highly efficient, reliable, and they generate very little sludge but their application is limited because of high costs, need for reliable power supply and for specialized personnel. On the other hand, although solar distillations is clean and inexpensive to run, colossal sum of capital required for the initial installation of solar units is a major impediment to its utilization. It appears therefore that adsorption is the most appropriate procedure for removal of fluoride from water, especially in less developed regions of the world because it is simple, inexpensive, and results in high quality of treated water [15–18].

Adsorption uses high surface area solid adsorbents which have exterior reactive sites at which, when the material is contacted with F-contaminated water, the contaminant F particles in the water can attach and be removed alongside the adsorbent at the time of phase separation. The most commonly used adsorbents for removal of fluoride from water include activated carbon (AC), activated alumina (AA), and commercial ion-exchange resins (IER). These adsorbents are normally characterized by high F adsorption capacities due to their porous structures and large surface areas but their application is limited due to high costs and they require frequent regeneration which complicates the process. Because the adsorbents are non-biodegradable and tend to persist in the environment for long periods of time [19], the spent waste from the process must carefully be disposed of. Because of these limitations a lot of unconventional adsorbents including various biosorbents [20–23] and a number of

Correspondence: E. W. Wambu, Department of Chemistry, Bondo University College, P.O. Box 210-40601, Bondo, Kenya
E-mail: wambuenos@yahoo.com

Abbreviations: **AA**, activated alumina; **AAS**, atomic absorption spectroscopy; **AC**, activated carbon; **EC**, electrocoagulation; **ED**, electrodialysis; **IER**, ion-exchange resins; **M**, siliceous mineral of a Kenyan origin; **pHznc**, point of zero net charge; **RO**, reverse osmosis

low-cost carbons [24–26] have been studied widely for use as substitute inexpensive adsorbents.

To prepare carbons for water defluoridation, organic materials, on average 3–5 times the required carbon mass, are needed for gasification and charring. Then the carbons obtained require high temperature treatment in the range of 800–1400 K, or some other form of activation to enhance their surfaces for F adsorption which makes them expensive to produce [15]. Biosorption uses animal and plant biomasses in powdered form ''as is'' without prior gasification into chars. However, the use of biosorbents is limited because the source organisms for certain F biosorbents may not be readily available in some regions of the world for ease use. Furthermore, biosorbents are liable to chemical and biological attack which reduces their scope and efficacy of application. A plausible adsorbent which is required for removal of F from water must be one that is: affordable, stable, and usable in a wide spectrum of water conditions without deterioration or fouling of treated water, one with attractive adsorptive capacities, easy enough to prepare and use and straightforward to regenerate or cleanse for the final disposal so that it does not pose undue environmental hazard.

Certain clays and soil minerals [17, 18, 27–29] have attracted a lot of research interest in the recent past as alternative adsorbents for F removal from water due to their attractive properties which include: ready and abundant availability, chemical stability, good natural adsorptive properties, ease of preparation for use, uncomplicated regeneration after use, and general environment passiveness [30–32]. In the present work, defluoridation capacity of a siliceous mineral from Kenya, M1, was studied in batch simulation tests. The effect of adsorption parameters including: time of contact, batch adsorbent loading, competing ions, pH, and temperature on F adsorption onto M1 was evaluated and equilibrium isotherms used to determine the adsorption capacity and to elucidate the mechanism for F adsorption. The batch adsorption results were then verified for practical application on high fluoride water from a natural source from Elementaita-Gilgil, Nakuru County, Kenya, using column experiments [33].

2 Experimental

2.1 Preparation of the materials

The mineral, M1, was collected from its natural deposits at Matili [00°44.90′N, 34°43.70′E; elevation: 1638 m] in Bungoma County, Kenya. It was air-dried and crushed to pass through <2 mm mesh. The crushed mineral was dispersed by mechanical treatment and sedimentation in de-ionized water to obtain <1 μm fractions. Eight portions of the mineral were soaked in 0.1 M HCl at 0.1 g/mL ratio and magnetically stirred for 30, 60, 90, 120, 150, 180, 210, and 420 min, respectively. After stirring, the samples were suction filtered, washed with excess de-ionized water and oven-dried at 382 K overnight. All the samples were assessed for their F uptake capacity at initial F concentration of 1000 mg/L, 293 K, and 0.1 g/mL adsorbent dosage and the results compared with those of non-acid treated mineral.

2.2 Characterizations of the materials

The chemical and mineralogical composition of the mineral adsorbent was determined using atomic absorption spectroscopy (AAS) and X-ray diffraction analysis, respectively. Loss on ignition (LOI) was determined by ashing the sample at 1273 K. The zero point of charge (pHznc) was determined by fast alkalimetric titration according to the method of Weng et al. [34] and the pH of the sample measured using Hanna Instruments pH-211-microprocessor pH meter in 1 M KCl by soaking 5 g of sample in 50 mL aliquots of the salt solution.

2.3 Batch adsorption experiments

Six portions (5 g each) of acid treated M1 were mixed with 50 mL aliquots of NaF solution containing 1000 mg/L F and shaken on a reciprocating shaker at 293 K for time intervals of 60, 120, 180, 240, 360, and 480 min, respectively. The experiments were repeated using 10, 15, 20, 25, and 30 g portions of the adsorbent in 50 mL of the adsorbate solution shaking the mixture for 120 min (which was the time required to reach the initial equilibrium). Parallel experiments were carried out using 25 g portions of M1 (which was the minimum mass of the material required for the initial equilibrium removal efficiency) in 50 mL aliquots of adsorbate solution containing 5, 10, 20, 50, 100, 200, 400, 800, and 1000 mg/L F ions at ambient pH 3.4 ± 0.2. This were then repeated at adsorbate pH values of 3, 4, 5, and 7 using 1000 mg/L F adsorbate solution. The pH of the solutions was adjusted as appropriate by addition of small amounts of 1 M NaOH or 1 M HCl using 50-μL burettes. All tests were carried out in triplicate at room temperature (293 K) and another set of tests carried out at ambient pH (3.4 ± 0.2) of the material using 1000 mg/L F concentration at 293, 303, 313, 323, and 333 K, respectively. The effect of selected anions (co-ions) was studied using 0.1 M respective potassium salts solutions containing 1000 mg/L F as the adsorbate solution at pH 3.4, 293 K, and adsorbent dosage of 0.5 g/mL. In all tests, phase separation was achieved by centrifugation and the supernatant fluoride concentration determined potentiometrically using a Tx EDT Model 3221 fluoride ion-selective electrode.

2.4 Up-flow column adsorption experiments

To verify defluoridation performance of M1 for practical applications, up-flow column adsorption experiments were carried out in Pyrex™ columns of about 1.0 cm id and 12 cm height at different fluoride concentrations (5–90 mg/L), bed depths (2–4 g), and flow rates (5–45 mL/min). The high F water samples were passed through columns from 5-L reservoirs at a height of 1 m above the columns. The effluent was collected at different time intervals (0–12 h) and analyzing for residual fluoride concentration using an ion-selective electrode as in Section 2.3.

3 Results and discussion

3.1 Chemical, surface, and mineralogical properties of the material

The summary of major characteristics of M1 is presented in Tab. 1.

The main minerals in the material were quartz, potassium tectoaluminotrisilicate and albite. Consequently, chemical analysis showed that alumino-silicates were the major constituents in the material. Such material would assume net negative surface charge because of the high density of electronegative oxygen atoms associated with the minerals. The negative charge would favor acid activation of the mineral for anionic adsorption as they easily protonate in acidic media increasing the surface positive charge and the adsorption potential for fluoride ions.

CLEAN Soil Air Water

Table 1. Major characteristics of M1 after pretreatment

Property	Value (%)
SiO_2	80.75%
Al_2O_3	10.73%
K_2O	3.93%
Na_2O	1.52%
Fe_2O_3	0.89%
CaO	0.81%
TiO_2	0.40%
LOI	1.91%
pH	3.4 ± 0.2
PHznc	3.8 ± 0.2
Main minerals	
Quartz, synth.	SiO_2
Potassium tecto-alumotrisilicate	$K(AlSi_3O_8)$
Albite, calcian, ordered	$(Na, Ca)Al(Si, Al)_3O_8$

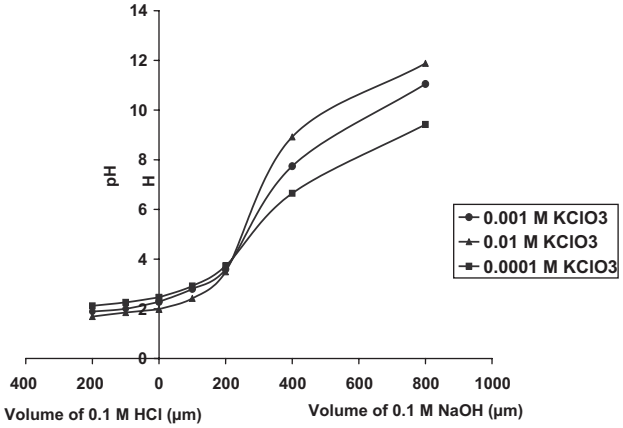

Figure 2. Determination of pHznc by fast alkalimetric titration in different concentrations of $KClO_3$.

3.2 Effect of acid activation

To optimize acid activation of the material for fluoride uptake, the effect of soaking the adsorbent in acid on its fluoride uptake was examined for different time intervals using 0.1 M HCl and the result is presented in Fig. 1.

There was no significant difference in adsorption capacity of 30- and 90-min acid-activated samples. The highest F removal efficiency was recorded using 3-h acid-activated samples. However, there was remarkable drop in the adsorption capacity of the material when time of contact of adsorbent with the acid was increased to 7 h indicating that prolonged acid exposure of the adsorbent results in irreversible deterioration of adsorption surface of the soil [15]. This means that this siliceous mineral could most effectively be activated for F adsorption at 3 h contact using 0.1 M HCl.

Thus, after acid activation, the pH of activated adsorbent was measured and the pH of zero net charge (pHznc) determined by fast alkalimetric titration and the results presented in Fig. 2. The pH of M1 was found to be 3.4 ± 0.2 and the pHznc was 3.8.

Alkalimetric titration involves adsorption of H^+ or OH^- at different concentrations (pH) and at different ionic strengths. The amphoteric nature of soil surfaces means that there is a pH at which the different curves intersect. At this point adsorption of protons is independent of ionic strength. This point approximates the pHznc of the material [34]. The acidic pH value was attributed to the activation procedure by the acid employed in this work and to the protonation of oxygen centers in the clay system. As expected, the acid-activated material had net positive charge on the surface which is favorable for anionic F adsorption [35].

3.3 Sorption experiments

Apart from the mineral and chemical composition of the adsorbent affecting adsorbent properties, the solution parameters play a major role in determining the performance of the adsorbent in an adsorptive system. The effect of pH, adsorbate concentration, adsorbent loading, competing ions, and temperature on M1 uptake of fluoride ions from aqueous media was investigated and the results discussed in the subsequent Sections 3.3.1–3.3.5.

3.3.1 Effect of adsorbate pH

The influence of change in pH on F adsorption was studied at pH values of 3, 4, 5, and 7. The results of these tests are presented in Fig. 3.

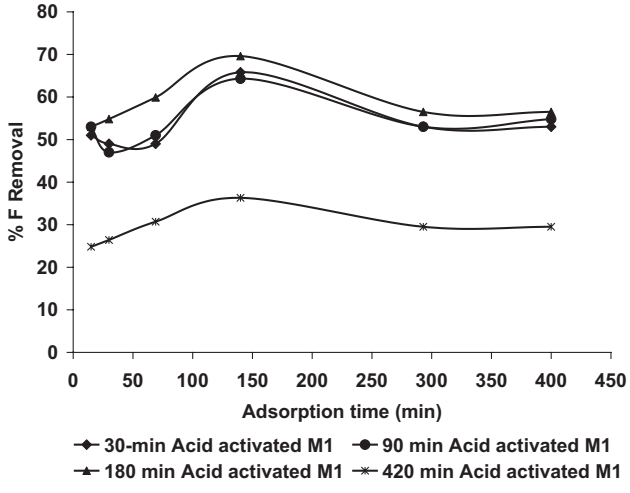

Figure 1. Effect of acid activation on M1 uptake of F ions from solution (initial F concentration = 1000 mg/L, Temperature = 293 K, Adsorbent dosage 0.1 g/mL).

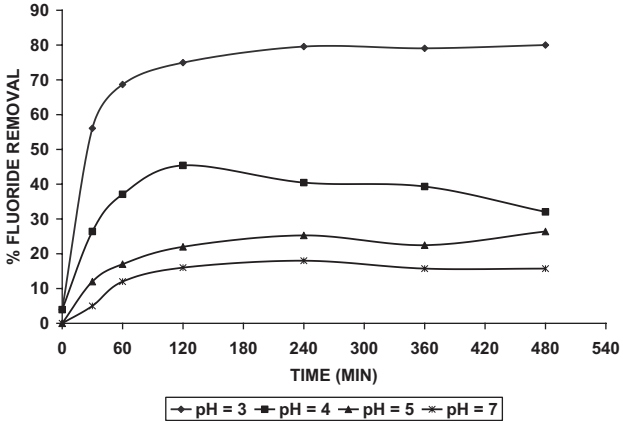

Figure 3. Effect of change in adsorbate pH on fluoride uptake by M1 at 293 K using 1000 mg/L F ion concentration at 0.1 g/mL adsorbent dosage, pH = 3, 4, 5, and 7.

The pH influenced adsorption of F onto M1 strongly. At pH 3 the adsorption equilibrium was attained rapidly indicating high affinity for F by M1 surfaces at low pH than at higher pH values. Highest adsorption (80%) occurred at low pH 3. The adsorption of F then declined rapidly with increasing pH to 40, 22 and then 18% when the pH was raised from 3 to 4, 5 and 7, respectively. It means that at low pH the adsorbent surface takes-up hydrogen ions from solution increasing the surface positive charge, affinity and adsorption capacity of M1 for F. At high pH, the H-ions desorb from the surface reducing the positive charge and resulting in low adsorptions of F. Thus highest F uptake is achieved at the low pH < 3 as also observed by Hamdi and Srasra [16].

3.3.2 Effect of adsorbent dosage

The effect of change in mass of M1 while maintaining initial concentration and volume of adsorbate F solution was constant then investigated and results presented in Fig. 4.

Percentage F removal initially increased very gradually then more rapidly when the amount of adsorbent was increased from 5 to 25 g/50 mL of adsorbate solution. Given the adsorption time requirement was quite low (70% adsorption in 5 min), it can be assumed that F adsorption onto M1 proceeds in two stages; the rapid initial adsorption utilizing high affinity surface sites, followed by gradual diffusion of the adsorbate into less exposed sites in the adsorbent. This indicates heterogeneity in adsorbent surfaces. Most efficient (≈90%) F removals were achieved with dosage ratio ≥1:2 g/mL. But as the amount of M1 was increased, the adsorption mixture became too thick to agitate effectively. This means that optimum removal of F could be achieved in M1 loading just about 0.5 g/mL ratio.

3.3.3 Effect of adsorbate concentration

The effect of initial F concentration on its removal from solution by M1 is illustrated in Fig. 5.

Close to 100% adsorption of F were recorded for initial F concentration up to 200 mg/L. The percentage F adsorption then declined between 200 and 400 mg/L F concentration to about 86% and thereafter remained more or less constant. This indicates that saturation of adsorbent sites do not take place at these concentrations. Instead, more adsorptive sites are generated as F^- ions adsorb leading to constant partition of the ion between the phases. This phenomenon

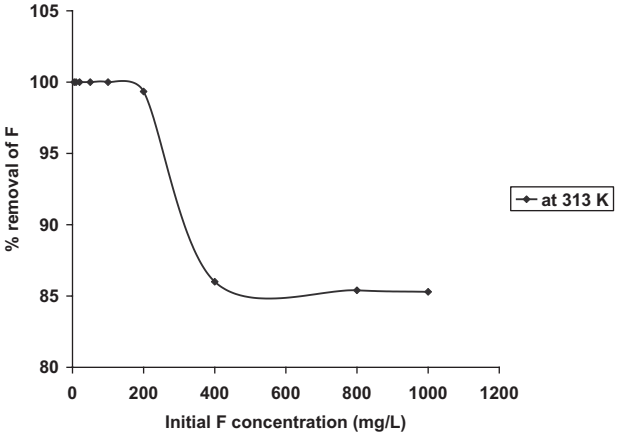

Figure 5. Effect of initial fluoride concentration on its percentage adsorption onto a siliceous mineral of a Kenyan origin.

is associated with high porosity and heterogeneity of the crystal structure of adsorbent and high affinity and penetrating power of the adsorbate particles [36]. It means that F^- ions are able to access adsorptive sites in the crystalline regions of the mineral which are not accessible to other particles in the aqueous system. The small size and large charge-to-volume ratio enable the ion to break inter-substrate bonds more easily and penetrate into the mineral structure in regions not already penetrated by the solvent. It would be expected that the action stops when more crystalline regions of the adsorbent are reached although this point is not attained at the present adsorbate concentrations. It shows that the material can be effectively utilized in defluoridation of aqueous solutions in the F contamination range of natural waters.

3.3.4 Effect of temperature

The effect of temperature was studied using 200 and 400 mg/L initial F concentrations. The results of these investigations are presented in Fig. 6.

The F uptake by M1 increased from 84% (for 400 mg/L) and 96% (for 200 mg/L) at 293 K to a peak at about 98 and 100% for temperature rise from 293 to 303 K and 323 K, respectively. It can be assumed that

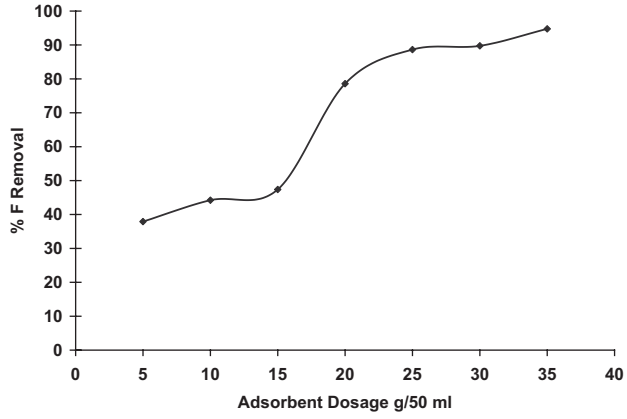

Figure 4. Effect of change in adsorbent dosage when varying amounts of M1 were agitated with 1000 mg/L for 2 h at 293 K.

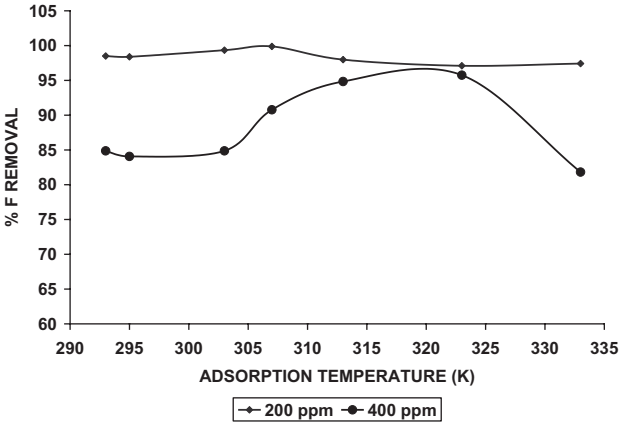

Figure 6. Effect of temperature on M1 adsorption capacity of fluoride ions at pH 3.4 and adsorbent dosage of 0.5 g/mL.

CLEAN Soil Air Water

increase in temperature provides the necessary activation energy that enables more F particles to interact effectively with the adsorptive sites in M1 resulting in higher adsorption. Thus, higher initial F concentrations required more energy hence, higher temperatures to reach their highest removal efficiency in agreement with results by Alagumuthu et al. [15]. However, at temperatures >323 K, F decreased because at this point the reacting particles cannot interact effectively due to increase in their kinetic energy and thermodecomposition of adsorption complexes resulting in reduced F adsorption. In general F could be removed from solution most efficiently at 303 K for lower concentrations (200 mg/L) and at 323 K at elevated concentrations (400 mg/L).

3.3.5 Effect of dissolved inorganic ions

The effect of dissolved inorganic anions was investigated and the results presented in Fig. 7.

Competing anions reduced M1 uptake of F. Reduction in F adsorption was in the order: chloride > nitrate > sulfate > dihydrogen phosphate. This suggests that the steric effects of the competing anions (chloride < nitrate < sulfate < dihydrogen phosphate) could be the main variable influencing the degree of competition for adsorbent sites between the anions and F ions. Smaller ions such chlorides have higher mobility through the aqueous matrix and penetrate adsorbent structure offering stronger competition for the adsorptive sites thereby reducing F adsorption more than sterically hindered oxyanions. For oxyanions, the affinity of anions for the adsorbent sites depends on the ratio of valency electron in the central atom to the number of oxygen atoms sharing into those valency electrons. This ratio is called the shared charge. Higher shared charge leads to lower affinity of an oxyanion and vice versa. The sulfate with a more electronegative sulfur center (higher share charge), draws electrons from the oxygen atoms making them poorer Lewis acid (electron donors). This makes the ion a poorer competitor for positive centers in the adsorbent surface than the nitrate for instance. Dihydrogen phosphate ion showed lower competitiveness for the sorptive sites than the sulfate. It can be assumed that the acid ion ionizes releasing hydrogen ions which adsorb on the adsorbent surface increasing its positive charge and the potential to adsorb F.

Nonetheless even with 0.1 M concentration of competing sulfate and nitrate ions; above those that could be found in natural water systems 80% F removal was achieved indicating that M1 would still be potent for use as a low-cost defluoridant.

3.4 Equilibrium analysis

To examine adsorption mechanisms and gain insight into the nature of the adsorbate–adsorbent interactions, equilibrium analysis was carried out and the results presented in Fig. 8.

The F adsorption isotherm could be classified as a type three high affinity (H3) isotherm, according to Giles classification of adsorption isotherms, based on the initial part of the curve being perpendicular to the concentration axis. Type H3 isotherm describe a system of high affinity for the solute by substrate [36]. The vertical initial portion of the curve indicate that the adsorbent has got such high affinity for the adsorbate that <200 mg/L F concentration, the ion is completely adsorbed, or at least there is no measurable amount remaining in solution. The H3 isotherm has been associated with adsorption of large units, such as ionic micelles or polymeric molecules, but single ions systems H-type isotherms are consistent with ion-exchange mechanisms where the adsorbate exchanges with others of much lower affinity for the surface. This indicates that anionic exchange protocol could the main adsorption mechanism in F adsorption on M1. The higher charge-to-volume ratio in F ions could also make them more energetically favored in the interaction with the substrate materials. This would be important for adsorption of F from aqueous streams in presence of other anions with larger spatial radius; selective removal of F being desirable.

The Linear Langmuir and Freundlich isotherms were also employed in the equilibrium analysis of F adsorption onto the clay mineral. The Langmuir Isotherm was used in its double reciprocal form as:

$$\frac{1}{q_{eq}} = \frac{1}{bq_{max}C_{eq}} + \frac{1}{q_{max}} \quad (1)$$

where C_{eq} is the equilibrium concentration (mg/L), q_{eq} the amount of metal ion sorbed (mg/g), q_{max} is q_{eq} for a complete monolayer coverage of the material by the adsorbate (mg/g), and b sorption equilibrium constant (L/mg). A plot of $1/q_{eq}$ versus $1/C_{eq}$ should indicate a straight line of slope $1/bq_{max}$ and an intercept of $1/q_{max}$ from which both the adsorption capacity q_{max} and the equilibrium constant b

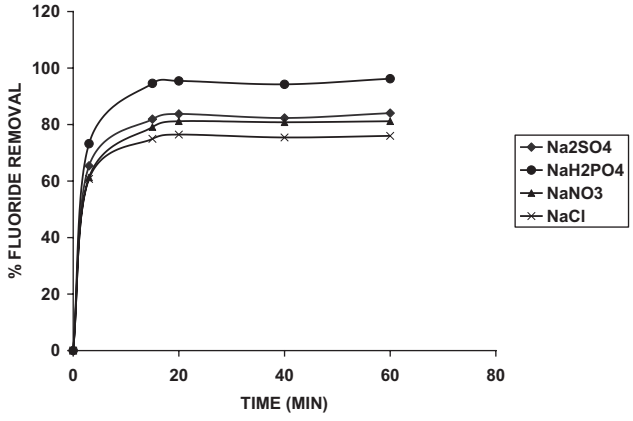

Figure 7. Effect of presence of selected co-ions on M1 adsorption capacity of fluoride ions from 1000 mg/L initial concentration at 303 K, pH 3.4, and adsorbent dosage of 0.5 g/mL.

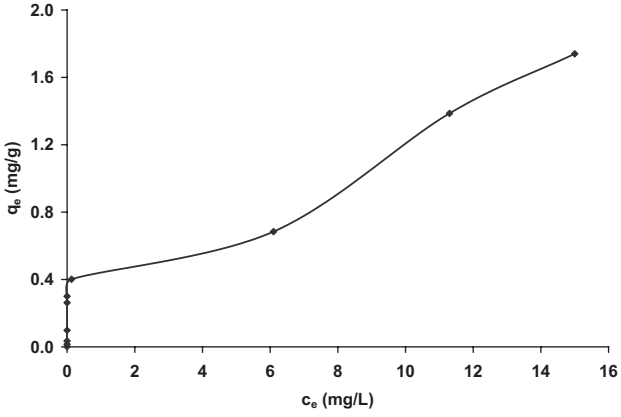

Figure 8. Adsorption isotherms for the removal of F ions from aqueous solution by M1 at 303 K and pH 3.4.

representing the thermodynamic stability of the adsorption constant between the surface and the solute can be determined.

On the other hand, the linearized Freundlich isotherm was adopted as:

$$\log q_{eq} = \log K_f + n \log C_{eq} \quad (2)$$

For this equation, the value of the constant n is characteristic of the intensity or loading of the adsorbate on the adsorbent surface whereas K_f is related to the equilibrium constant of the adsorption process and therefore indicative of the affinity of the adsorbent for the adsorbate particles. A plot of $\log q_{eq}$ against $\log C_{eq}$ is a linear graph of gradient n and vertical intercept equal to $\log K_f$.

Both the Langmuir and the Freundlich adsorption isotherms were employed in equilibrium description of F adsorption onto M1 and the results presented in Fig. 9a and b. The Langmuir and Freundlich isothermal parameters were computed from the linear plots and compared with those of other low-cost adsorbents and presented in Tab. 2.

The Langmuir and Freundlich isotherms fitted well the adsorption data with R^2 values of 0.9991 and 0.9934, respectively; showing that F adsorption on M1 could be described by these models. The values of affinity coefficient, K_f, and intensity parameter, n, of the Freundlich model indicated effective binding of adsorbate particles by M1 surfaces.

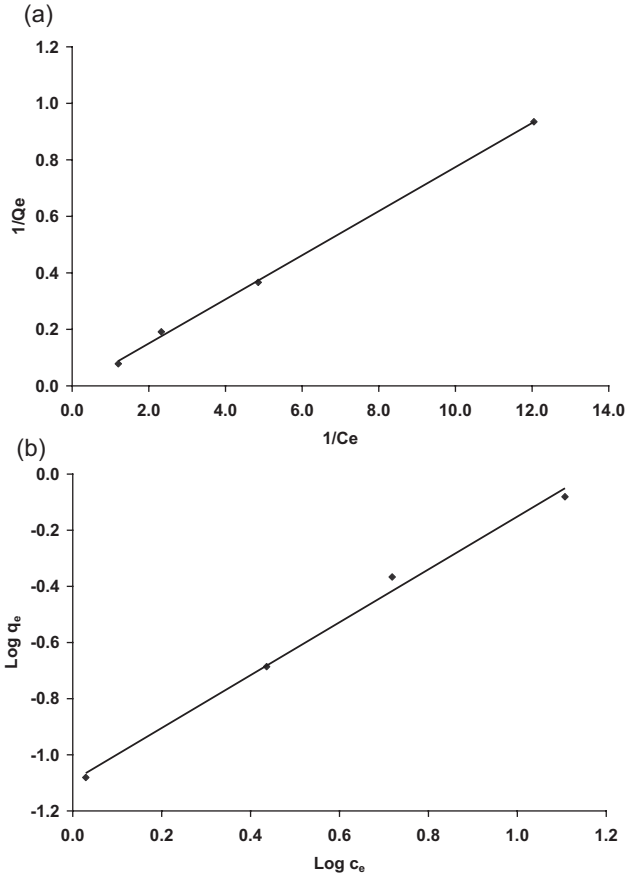

Figure 9. (a) The Langmuir isotherm for the adsorption of F onto M1, (b) The Freundlich isotherms for the adsorption of F onto M1.

A total of 50 low-cost F adsorbents from the literature were considered in the comparisons. It could be noted that on average IERs had the highest F adsorption capacities (61.57 mg/g) reported in literature, followed by alumino-silicate minerals (36.6 mg/g), ferric minerals (25.22 mg/g), siliceous/silicate minerals (14.10 mg/g), biosorbents (5.66 mg/g), low-cost ACs (5.20 mg/g), alumina-based adsorbents (4.28 mg/g), calcareous minerals (2.79 mg/g), carbonaceous minerals (2.65), and phosphate minerals (2.51 mg/g), respectively. These classes of low-cost adsorbents are not clear-cut and for mineral adsorbents, one adsorbent may belong to several classes. It was found that activated silica and IERs have F adsorption capacities well above that of M1. However, apart from bone char and carbonaceous materials from coffee husks, F adsorption capacity of M1 was superior to those of biosorbents, carbonaceous adsorbents and alumina-based adsorbents considered in these comparisons. Although a number of minerals including: modified hematite, tourmaline, palygorskite clay, smectic clay, illito-kaolinites, kaolinite-ferrihydrite associate, and a ferric poly mineral from Kenya had better F sorption capacity when compared to M1, the F adsorption capacity of M1 was quite high compared to that of lateritic mineral, lignite, hydroxyapatite, Boehmite, fluorspar, Chinese red soil, calcite, pumice, quartz, activated kaolinite, and montmorillonites.

Differences in F adsorption capacities of adsorbents arise from differences in the chemical, structural, and surface properties of adsorbents and from adsorption parameters including: concentration, pH, temperature, ionic strength, counter ions, co-ions, rate of agitation, speciation, and time of contact, etc., employed in the adsorption tests. Remarkable F adsorption characteristics depicted by M1 in this work shows that the mineral could be utilized as an inexpensive defluoridation media for practical removal of F from water. Besides, the mineral can be obtained cheaply from its abundant natural deposits for easy and safe use as F adsorbent.

3.5 Verification of defluoridation performance of M1 on real water

To verify the performance of M1 for practical applications in defluoridation of water, up-flow column adsorption experiments were conducted in Pyrex™ columns using high F water samples containing about 5–90 mg/L F from natural sources in Elementaita-Gilgil Area, Nakuru County, Kenya [33]. The fluoride adsorption data from the column experiments were then analyzed using the Thomas model [58] in the form:

$$\log\left[\left(\frac{C_0}{C_v}\right) - 1\right] = \frac{K_{Th} q_0 m}{Q} - \frac{K C_0 V}{Q} \quad (3)$$

where, C_0 and C_v are the influent and effluent concentration (mg/L), K_{Th} is the Thomas rate constant, q_0 is maximum F adsorption capacity of M1 in the column test, m is the adsorbent mass in column (g), Q is influent flow rate (mL/min), and V is throughput volume (mL). The Thomas rate constant, K_{Th}, and the maximum adsorption capacity, q_0, values were computed from the slope and intercept of linear plot of $\log[(C_0/C_v) - 1]$ versus V for various column adsorption conditions. The F breakthrough curve for 89 mg/L F water and the Thomas rate constant, K_{Th}, and maximum adsorption capacity, q_0, values for different column operating conditions are depicted in Fig. 10 and in Tab. 3, respectively.

The M1 breakthrough curve was typical ''S-shaped'' curve. Figure 10 shows that at an average flow rate of 9.9 mL/min, nearly

CLEAN Soil Air Water

Table 2. Langmuir and Freundlich isotherm constants for the adsorption of F onto M1 compared with those of other low-cost F adsorbents in literature

Adsorbent and source	pH, Temp (K)	Langmuir		Freundlich	Reference
		Q_{max} (mg/g)	b (L/mg)	K_f	
Aluminum hydroxide modified hematite	2.3–6.3, ng[a]	116.75	0.0256	4.7521	[17]
Tourmaline	ng, 298	98	0.02	0.62	[18]
Palygorskitic clay	3.0, 298	93.45	0.0049	0.6	[27]
Smectic clay	3.0, 298	84.03	0.0043	0.52	[27]
Chitin/cellulose composite	6.5, 303	83.75	0.0088	1.6417	[37]
Glutaraldehyde cross-linked calcium alginate	8.0, 298	75.5	0.006	0.496	[38]
Illito-kaolinitic clay	3.0, 298	69.44	0.0042	0.48	[27]
Modified silica	4.0, ng	44.4	0.01	0.42	[28]
Modified attapulgite	ng, 305	41.5	0.0143	1.51	[39]
Bone char	ng, 298	29	0.02	0.76	[18]
Carbonaceous materials from coffee husks	ng, 298	26.8	0.17	5.9	[40]
La(III)-Amberlite 200CT resin	6.0, 303	25.46			[41]
Ferrihydrite	5.5, 298	20	0.323	6.58	[29]
Cynodon dactylon	1.0, 298	16.32	0.138	0.41	[20]
Kaolinite–ferrihydrite associate	5.5, 298	12.83	0.054	1.58	[29]
Ferric polymineral from Kenya	3.4, 303	12.7	1.38	4.73	[30]
Siliceous mineral	3.4, 303	12.25	0.00637	0.0807	This work
Lateritic mineral from Kenya	3.4, 303	10.4792	0.0524	0.6322	[31]
Bismuth aluminate	ng, 323	9.43	0.24	1.85	[42]
Commercial activated alumina	6.8, ng	7.692	0.13	0.83	[23]
Phyllanthus emblica activated carbon	7.0, 298	7.172	2.075	4.357	[24]
Lignite	ng, 298	6.9	0.2134	1.1473	[43]
Tamarind seed biosorbent	7.0, 293	6.37	0.69	–	[21]
Carbonaceous materials from pyrolysis of sewage sludge	5.3, ng	6.2	0.037	0.28	[25]
Thermally activated carbon	7.0, 303	4.617	1.58	3.024	[15]
Hydroxyapatite	6.0, ng	4.54	2.44	10.5	[44]
Lewatit FO 36 resin	5.5, 298	4.2918	0.231	3.467	[45]
Stone dust–alumina mixture	6.5, 300	4.009	3.3338	2.8436	[46]
South Moravian lignite	ng, 303	3.73	13.7	0.01	[26]
Fine coke	ng, 303	3.43	0.141	0.6287	[26]
Aluminum titanate	ng, 323	3.35	0.11	0.52	[42]
Boehmite	4.2, ng	2.057	0.2806	0.574	[47]
Fluorspar	6.0, ng	1.79	0.091	0.15	[44]
Aluminum sulfate	7.0, 293	1.7142	0.3744	1107.67	[48]
Synthetic siderite	ng, 298	1.713	0.202	0.2761	[49]
Montimorrillonites	ng, 303	1.485	4.22	0.279	[50]
Kaolinites	5.5, 298	1.45	0.143	0.47	[29]
Brick powder	6.8, ng	1.345	0.43	0.42	[23]
Algal *Spirogyra* 101 biosorbent	–	1.272	585	–	[22]
Activated quartz	6.0, ng	1.16	0.086	0.1	[44]
Egg-shell powder	6.0, 303	1.09	0.448	0.368	[51]
Activated charcoal	2.0, 302	1.076	0.429	0.312	[52]
Red soil of China	6.0, 300	0.8545	0.0609	0.1104	[53]
Bituminous coke	ng, 303	0.786	0.0327	0.0611	[26]
Synthetic hydroxyl apatite	2.0, 298	0.489	42.454	0.371	[54]
Calcite	6.0, ng	0.39	0.023	0.066	[44]
Pumice	7.0, ng	0.31	0.97	0.85	[55]
Lanthanum oxide		0.2503	0.0077	0.21	[56]
Quartz	6.0, ng	0.19	0.12	0.023	[44]
Tea leaves biomass	6.8, ng	0.054	0.34	0.01	[23]
Acid-activated kaolinites	4.0, 313	0.045	2.7	1.287	[57]

90% fluoride removal was recorded in the initial 17 mL of effluent solution. Then the influent fluoride concentration increased and remained constant at 89 mg/L after about 56 mL of effluent solution. The Thomas model fitted the adsorption data with $R^2 > 0.93$ at all bed heights and flow rates. The values of q_0 predicted by the Thomas model were consistent with Langmuir adsorption capacity predicted in Section 3.5 showing that the Thomas model could describe sorption of fluoride onto M1. The Langmuir capacity was however somehow better because agitation in batch system increases surface accessibility to adsorbate ions above that in stationary column phase. At constant m the value of K_{Th} decreased with decreasing flow rate, Q, and decreasing influent concentration, C_0, while q_0 was enhanced at lowest flow rates, Q, and lowest F concentrations, C_0. Similar findings have been reported for alumina cement granules [59, 60], Kanuma mud [59, 60], and magnesia-loaded fly ash cenospheres [61]. High adsorption capacity of M1 shows that the adsorption process is not affected by real water aqueous matrix in the water used in this work and therefore this mineral, M1, could be used to scavenge F from real water situations.

Table 3. Column sorption data of fluoride onto M1 at different experimental conditions

m (g)	C_0 (mg/L)	Q (mL/min)	K_{Th} (L/mg/min)	q_0 (mg/g)
2	899	44.84	0.1345	244.17
4	89	9.26	0.0117	560.22
4	17	5.32	0.2867	9.77
4	8	5.32	0.1409	11.67

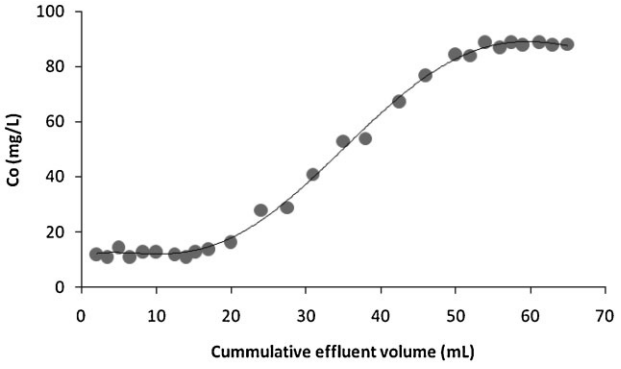

Figure 10. Column breakthrough curves at a dose of 4.0 g of M1 and at 90 mg/L influent fluoride concentrations at a flow rate of 9.9 mL/min.

4 Concluding remarks

In this work, F adsorption onto M1, a siliceous mineral of a Kenyan origin, was studied in batch and fixed-bed column adsorption systems. Fluoride adsorption onto M1 was a fast process with the initial batch equilibrium being attained within 20 min. The adsorption temperature and adsorbate pH were the main variables determining the adsorption characteristics of F on M1 in a batch system. In general, the adsorption capacities increased with increasing temperature and decreasing solution pH. Close to 100% F removal was realized using initial F concentration of 200 mg/L at 0.5 g/mL adsorbent dosage, 303–333 K temperature and pH 3.4 ± 0.2 and the adsorption isotherm could be classified as H3 type according to Giles classification and the equilibrium adsorption could be described by both the Langmuir and Freundlich adsorption models. The maximum Langmuir adsorption capacity was found to be 12.4 mg/g. Although the batch adsorption efficiency reduced in presence of competing ions such as the chlorides, nitrates, and sulfates this study has demonstrated that fluoride ions could be removed from aqueous solutions using a siliceous mineral, M1 as a low cost adsorbent. The fixed-bed column studies were conducted at different flow rates, bed depth, and initial fluoride concentration. The fluoride removal by a fixed bed of M1 using different flow rates and adsorbent column loadings could be described be the Thomas Model. F could be removed most efficiently at low influent F concentration and lowest flow rates. In general the findings in this work have demonstrated that M1 could be used to remove F from water as an alternative low-cost adsorbent.

Acknowledgments

This study was funded by the International Foundation for Sciences (IFS) and the National Council for Science and Technology (NCST-Kenya).

The authors have declared no conflict of interest.

References

[1] WHO (World Health Organization), *Guidelines for Drinking Water Quality*, World Health Organization, Geneva **2004**.

[2] A. K. Chaturvedi, K. P. Yadava, K. C. Pathak, V. N. Singh, Defluoridation of Water by Adsorption on Fly-Ash, *Water Air Soil Pollut.* **1990**, *49*, 51.

[3] J. P. Shorter, J. Massawe, N. Parry, R. W. Walker, Comparison of Two Village Primary Schools in Northern Tanzania Affected by Fluorosis, *Int. Health* **2010**, *2*, 269.

[4] R. W. Kahama, D. N. Kariuki, H. N. Kariuki, L. W. Njenga, Fluorosis in Children and Sources of Fuoride Around Lake Elmentaita Region of Kenya, *Fluoride* **1997**, *30*, 19.

[5] R. S. Dave, D. G. Acharya, S. D. Vediya, M. T. Machhar, Status of Fluoride in Ground Water of Several Villages of Modasa Taluka, North Gujarat for Drinking Purpose, *Der. Pharma Chem.* **2010**, *2*, 237.

[6] F. J. Gumbo, G. Mkongo, Water Defluoridation for Rural Fluoride Communities Affected in Tanzania, in *Proceedings of the 1st International Workshop on Fluorosis Prevention and Defluoridation of Water held at Ngurdoto in Tanzania on October 18–21, 1995* (Eds: E. Dahi, H. Bregnhøj), The International Society for Fluorosis Prevetion Research, Dunedin, New Zealand **1995**, p. 109.

[7] S. Vasudevan, J. Lakshmi, G. Sozhan, Studies on a Mg–Al–Zn Alloy as an Anode for the Removal of Fluoride from Drinking Water in an Electrocoagulation Process, *Clean – Soil Air Water* **2009**, *37 (4–5)*, 372.

[8] E. I. Reardon, Y. X. Wang, A Limestone Reactor for Fluoride Removal from Wastewater, *Environ. Sci. Technol.* **2000**, *34*, 3247.

[9] KEBS (Kenya Bureau of Standards), *Report on Kenya's High Fluoride Levels in Drinking Water: Excess Fluoride in Water in Kenya*, Consultative Committee Kenya Bureau of Standards, Nairobi **2010**.

[10] C. Y. Hu, S. L. Lo, W. H. Kuan, Effects of the Molar Ratio of Hydroxide and Fluoride to Al(III) on Fluoride Removal by Coagulation and Electrocoagulation, *J. Colloid Interface Sci.* **2005**, *283*, 472.

[11] M. B. S. Ali, B. Hamrouni, M. Dhahbi, Electrodialytic Defluoridation of Brackish Water: Effect of Process Parameters and Water Characteristics, *Clean – Soil Air Water* **2010**, *38 (7)*, 623.

[12] P. Sehn, Fluoride Removal with Extra Low Energy Reverse Osmosis Membranes: Three Years of Large Scale Field Experience in Finland, *Desalination* **2008**, *223*, 73.

[13] L. Anjaneyulu, E. A. Kumar, R. Sankannavar, K. K. Rao, Defluoridation of Drinking Water and Rainwater Harvesting Using a Solar Still, *Ind. Eng. Chem. Res.* **2012**, *51*, 8040.

[14] C. Castel, M. Schweizer, M. O. Simonnot, M. Sardin, Selective Removal of Fluoride Ions by a Two-Way Ion-Exchange Cyclic Process, *Chem. Eng. Sci.* **2000**, *55*, 987.

[15] G. Alagumuthu, V. Veeraputhiran, R. Venkataraman, Adsorption Isotherms on Fluoride Removal: Batch Techniques, *Arch. Appl. Sci. Res.* **2010**, *2*, 170.

[16] N. Hamdi, E. Srasra, Removal of Fluoride from Acidic Wastewater by Clay Mineral: Effect of Solid–Liquid Ratios, *Desalination* **2007**, *207*, 238.

[17] A. Teutli-Sequeira, M. Solache-Ríos, P. Balderas-Hernández, Modification Effects of Hematite with Aluminum Hydroxide on the Removal of Fluoride Ions from Water, *Water Air Soil Pollut.* **2012**, *223*, 319.

[18] W. Ma, F. Ya, R. Wang, Y. Zhao, Fluoride Removal from Drinking Water by Adsorption Using Bone Char as a Biosorbent, *Int. J. Environ. Technol. Manage.* **2008**, *9*, 59.

[19] S. K. Nath, R. K. Dutta, Enhancement of Limestone Defluoridation of Water by Acetic and Citric Acids in Fixed Bed Reactor, *Clean – Soil Air Water* **2010**, *38 (7)*, 614–622.

[20] J. Samusolomon, P. M. Devaprasath, Removal of Alizarin Red S (Dye) from Aqueous Media by Using *Cynodon dactylon* as an Adsorbent, *J. Chem. Pharm. Res.* **2011**, *3*, 478.

[21] M. Murugan, E. Subramanian, Studies on Defluoridation of Water by Tamarind Seed, an Unconventional Biosorbent, *J. Water Health* **2006**, *4*, 453.

[22] S. V. Mohan, S. V. Ramanaiah, B. Rajkumar, P. N. Sarma, Biosorption of Fluoride from Aqueous Phase onto Algal *Spirogyra* IO1 and Evaluation of Adsorption Kinetics, *Bioresour. Technol.* **2007**, *98 (5)*, 1006.

[23] G. R. Munavalli, V. K. Patki, A Comparative Study of Defluoridation Techniques, *J. Inst. Public Health Eng. India* **2009**, *10*, 35.

[24] V. Veeraputhiran, G. Alagumuthu, Sorption Equilibrium of Fluoride onto *Phyllanthus emblica* Activated Carbon, *Int. J. Res. Chem. Environ.* **2011**, *1*, 42.

[25] S. Márquez-Mendoza, M. Jiménez-Reyes, M. Solache-Ríos, E. Gutiérrez-Segura, Fluoride Removal from Aqueous Solutions by a Carbonaceous Material from Pyrolysis of Sewage Sludge, *Water Air Soil Pollut.* **2012**, *223 (5)*, 1959–1971.

[26] A. Sivasamy, K. P. Singh, D. Mohan, M. Maruthamuthu, Studies on Defluoridation of Water by Coal-Based Sorbents, *J. Chem. Technol. Biotechnol.* **2001**, *76*, 717.

[27] N. Hamdi, E. Srasra, Retention of Fluoride from Industrial Acidic Wastewater and NaF Solution by Three Tunisian Clayey Soils, *Fluoride* **2009**, *42*, 39–345.

[28] Y. Vijaya, A. Krishnaiah, Sorptive Response Profile of Chitosan Coated Silica in the Defluoridation of Aqueous Solution, *Electron. J. Chem.* **2009**, *6*, 713.

[29] S. Wei, W. Xiang, Surface Properties and Adsorption Characteristics for Fluoride of Kaolinite, Ferrihydrite and Kaolinite-Ferrihydrite Association, *J. Food Agric. Environ.* **2012**, *10*, 923.

[30] E. W. Wambu, C. O. Onindo, W. Ambusso, G. K. Muthakia, Equilibrium Studies of Fluoride Adsorption onto a Ferric Polymineral from Kenya, *J. Appl. Sci. Environ. Manage.* **2012**, *16 (1)*, 5.

[31] E. W. Wambu, C. O. Onindo, W. J. Ambusso, G. K. Muthakia, Fluoride Adsorption onto an Acid Treated Lateritic Mineral from Kenya: Equilibrium Studies, *Afr. J. Environ. Sci. Technol.* **2012**, *5*, 160.

[32] S. K. Nath, R. K. Dutta, Enhancement of Limestone Defluoridation of Water by Acetic and Citric Acids in Fixed Bed Reactor, *Clean – Soil Air Water* **2010**, *38 (7)*, 614.

[33] E. W. Wambu, G. K. Muthakia, High Fluoride Water in the Gilgil Area of Nakuru County, Kenya, *Fluoride* **2011**, *44 (1)*, 37.

[34] C. H. Weng, C. Z. Tsai, S. H. Chu, Y. C. Sharma, Adsorption Characteristics of Copper(II) onto Spent Activated Clay, *Sep. Purif. Technol.* **2007**, *54*, 187.

[35] E. M. Martinez, M. B. McBride, Comparison of the Titration and Ion Adsorption Methods for Surface Charge Measurement in Oxisols, *Soil Sci. Soc. Am. J.* **1989**, *53*, 1040.

[36] C. H. Giles, T. H. Macewan, S. N. Nakhwa, D. Smith, Studies in Adsorption. Part XI. A System of Classification of Solution Adsorption Isotherms and Its Use in Diagnosis of Adsorption Mechanisms and in Measurement of Specific Surface Areas of Solids, *J. Chem. Soc.* **1960**, 3973.

[37] G. Jayapriya, R. Ramya, X. R. Rathinam, P. N. Sudha, Equilibrium and Kinetic Studies of Fluoride Adsorption by Chitin/Cellulose Composite, *Arch. Appl. Sci. Res.* **2011**, *3 (3)*, 415.

[38] Y. Vijaya, S. R. Popuri, A. S. Reddy, A. Krishnaiah, Synthesis and Characterization of Glutaraldehyde-Crosslinked Calcium Alginate for Fluoride Removal from Aqueous Solutions, *J. Appl. Polym. Sci.* **2011**, *120*, 3443.

[39] J. Zhang, S. Xie, Y. S. Ho, Removal of Fluoride Ions from Aqueous Solution Using Modified Attapulgite as Adsorbent, *J. Hazard. Mater.* **2009**, *165*, 218.

[40] F. Ogata, H. Tominaga, H. Yabutani, N. Kawasaki, Removal of Fluoride from Water by Adsorption onto Carbonaceous Materials Produced from Coffee Grounds, *J. Oleo Sci.* **2011**, *60*, 619.

[41] L. Fang, K. N. Ghimire, M. Kuriyama, K. Inoue, K. Makino, Removal of Fluoride Using Some Lanthanum(III)-Loaded Adsorbents with Different Functional Groups and Polymer Matrices, *J. Chem. Technol. Biotechnol.* **2003**, *78*, 1038.

[42] M. Karthikeyan, K. P. Elango, Removal of Fluoride from Water Using Aluminium Containing Compounds, *J. Environ. Sci.* **2009**, *21*, 1513.

[43] M. Pekař, Affinity of the South Moravian Lignite for Fluoride Anion, *Pet. Coal* **2006**, *48*, 1.

[44] X. Fan, D. J. Parker, M. D. Smith, Adsorption Kinetics of Fluoride on Low-Cost Materials, *Water Res.* **2003**, *37*, 4929.

[45] M. R. Boldaji, A. H. Mahvi, S. Dobaradaran, S. S. Hosseini, Evaluating the Effectiveness of a Hybrid Sorbent Resin in Removing Fluoride from Water, *Int. J. Environ. Sci. Technol.* **2009**, *6 (4)*, 629.

[46] I. M. Umlong, B. Das, R. R. Devi, K. Borah, L. B. Saikia, P. K. Raul, S. Banerjee, L. Singh, Defluoridation from Aqueous Solution Using Stone Dust and Activated Alumina at a Fixed Ratio, *Appl. Water Sci.* **2012**, *2*, 29.

[47] J. Jiménez-Becerril, M. Solache-Ríos, I. García-Sosa, Fluoride Removal from Aqueous Solutions by Boehmite, *Water Air Soil Pollut.* **2012**, *223*, 1073.

[48] R. N. Yadav, O. P. Singh, R. Yadav, Study of the Aluminum Ammonium Sulphate as Defluoridated Agent in Drinking Water Earthenware, *Arch. Appl. Sci. Res.* **2010**, *2 (3)*, 11.

[49] Q. Liu, H. Guo, Y. Shan, Adsorption of Fluoride on Synthetic Siderite from Aqueous Solution, *J. Fluorine Chem.* **2010**, *131*, 635.

[50] G. Karthikeyan, A. Pius, G. Alagumuthu, Fluoride Adsorption Studies of Montmorillonite Clay, *Indian J. Chem. Technol.* **2005**, *12*, 263.

[51] R. Bhaumik, N. K. Mondal, B. Das, P. Roy, K. C. Pal, C. Das, A. Banerjee, J. K. Datta, Eggshell Powder as an Adsorbent for Removal of Fluoride from Aqueous Solution: Equilibrium, Kinetic and Thermodynamic Studies, *Electron. J. Chem.* **2012**, *9 (3)*, 1457.

[52] A. R. Tembhurkar, S. Dongre, Studies on Fluoride Removal Using Adsorption Process, *J. Environ. Sci. Eng.* **2006**, *48*, 151.

[53] M. X. Zhu, K. Y. Ding, X. Jiang, H. H. Wang, Investigation on Co-sorption and Desorption of Fluoride and Phosphate in a Red Soil of China, *Water Air Soil Pollut.* **2007**, *183*, 455.

[54] S. Gao, R. Sun, Z. Wei, H. Zhao, H. Li, F. Hu, Size-Dependent Defluoridation Properties of Synthetic Hydroxyapatite, *J. Fluorine Chem.* **2009**, *130*, 550.

[55] M. Malakootian, M. Moosazadeh, N. Yousefi, A. Fatehizadeh, Fluoride Removal from Aqueous Solution by Pumice: Case Study on Kuhbonan Water, *Afr. J. Environ. Sci. Technol.* **2011**, *5*, 299.

[56] C. Rao, J. Karthikeyan, Removal of Fluoride from Water by Adsorption onto Lanthanum Oxide, *Water Air Soil Pollut.* **2012**, *223*, 1111.

[57] P. K. Gogoi, R. Baruah, Fluoride Removal from Water by Adsorption on Acid-Activated Kaolinites, *Indian J. Chem. Technol.* **2008**, *15*, 500.

[58] H. C. Thomas, Heterogeneous Ion Exchange in a Flowing System, *J. Am. Chem. Soc.* **1944**, *66*, 1664–1666.

[59] S. Ayoob, A. K. Gupta, A. B. Basheer, A Fixed Bed Sorption System for Defluoridation of Ground Water, *J. Urban Environ. Eng.* **2009**, *3 (1)*, 17–22.

[60] N. Chen, Z. Zhang, C. Feng, M. Li, R. Chen, N. Sugiura, Investigations on the Batch and Fixed-Bed Column Performance of Fluoride Adsorption by Kanuma Mud, *Desalination* **2011**, *268*, 76–82.

[61] X. Xu, Q. Li, H. Cui, J. Pang, H. An, W. Wang, J. Zhai, Column-Mode Fluoride Removal from Aqueous Solution by Magnesia-Loaded Fly Ash Cenospheres, *Environ. Technol.* **2011**, *1*, 1–7.